FEBS Letters 588 (2014) 3621–3630

journal homepage: www.FEBSLetters.org

Review

Ultrastable atomic force microscopy: Improved force and positional stability

Allison B. Churnside [a], Thomas T. Perkins [a,b,*]

[a] JILA, National Institute of Standards and Technology and University of Colorado, Boulder, CO 80309, USA
[b] Department of Molecular, Cellular, and Developmental Biology, University of Colorado, Boulder, CO 80309, USA

ARTICLE INFO

Article history:
Received 4 March 2014
Revised 18 April 2014
Accepted 23 April 2014
Available online 4 May 2014

Edited by Elias M. Puchner, Bo Huang, Hermann E. Gaub and Wilhelm Just

Keywords:
Atomic force microscope
Force spectroscopy
Single-molecule biophysics
Force precision
Force stability

ABSTRACT

Atomic force microscopy (AFM) is an exciting technique for biophysical studies of single molecules, but its usefulness is limited by instrumental drift. We dramatically reduced positional drift by adding two lasers to track and thereby actively stabilize the tip and the surface. These lasers also enabled label-free optical images that were spatially aligned to the tip position. Finally, sub-pN force stability over 100 s was achieved by removing the gold coating from soft cantilevers. These enhancements to AFM instrumentation can immediately benefit research in biophysics and nanoscience.

Published by Elsevier B.V. on behalf of the Federation of European Biochemical Societies.

1. Introduction

Single-molecule atomic force microscopy (AFM) is providing a new window into fundamental questions in biophysics [1–11]. Few other techniques provide the ability to touch and manipulate matter on a nanometer scale as well as operate in a variety of conditions. As a result, AFM can probe individual biomolecules (DNA, RNA, and protein) in their native liquid environments. Despite more than two decades of biophysical research using AFM [12,13], important technical advancements are still expanding the range of science enabled by AFM.

At its core, AFM consists of a sharp tip interacting with a sample, creating a force [14]. The tip is mounted on a soft cantilever, so that the applied force bends the cantilever. This bending is typically measured by reflecting a laser beam off the back side of the cantilever onto a position-sensitive photodetector [15]. This detection scheme is known as an optical lever arm because a small displacement of the cantilever is magnified up to a relatively large motion of the beam on the detector, analogous to a mechanical lever. The optical lever is the predominant detection scheme due to its ease of use, although more complex detection schemes exist [16]. Most biological AFM experiments fall into one of two categories (imaging or force spectroscopy [3]) with emerging applications integrating AFM with chemical imaging modalities.

Imaging was the original application of AFM [14]. Early experiments utilized contact mode imaging where the tip was dragged at constant applied force along the surface, applying large lateral forces that could damage soft biological materials or the tip itself. A gentler imaging mode, known as tapping mode, was soon developed [17,18]. In this mode, the cantilever is vertically vibrated near its resonance frequency, minimizing lateral force by touching the sample only during a small portion of the sinusoidal cycle. Analysis of the phase, the frequency, and the amplitude of these oscillations provides new types of information beyond the simple topography of the sample [19–21].

AFM imaging continues to provide new insights into the structure and dynamics of biological systems that are difficult to discern by other biophysical techniques. For example, the large-scale organization of membrane proteins can be resolved in their native lipid bilayer (Fig. 1A) [22]. The resolution of these images is sufficiently high (0.6 nm) that they have been combined with crystallographic data using freely available software (DockAFM [23]) to deduce the

Abbreviations: AFM, atomic force microscopy; US-AFM, ultrastable atomic force microscopy; TERS, tip-enhanced Raman scattering; SMFS, single molecule force spectroscopy; bR, bacteriorhodopsin

* Corresponding author at: Department of Molecular, Cellular, and Developmental Biology, University of Colorado, Boulder, CO 80309, USA. Fax: +1 303 492 5235.
E-mail address: tperkins@jila.colorado.edu (T.T. Perkins).

http://dx.doi.org/10.1016/j.febslet.2014.04.033
0014-5793/Published by Elsevier B.V. on behalf of the Federation of European Biochemical Societies.

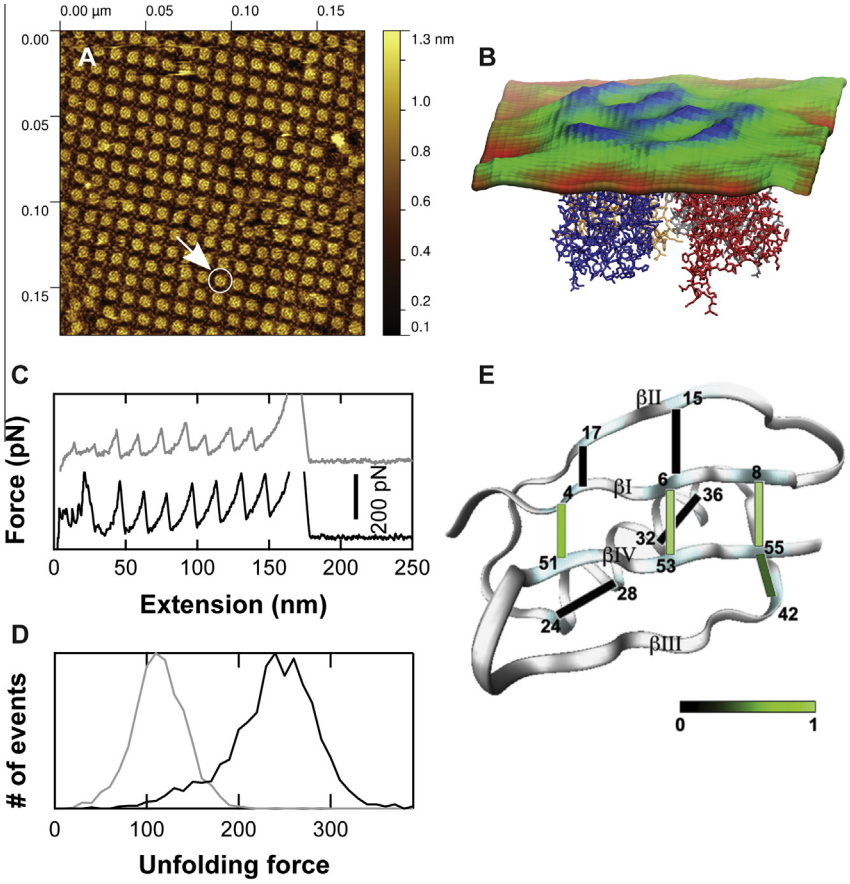

Fig. 1. Imaging and force spectroscopy of biomolecules. (A) A topographic image of *Escherichia coli*'s aquaporin Z, a water channel, reveals its lattice-like organization in the membrane (adapted from [22]). (B) The crystal structures of aquaporin Z can be docked to the high-resolution AFM image, bridging the gap between atomic structural information and larger scale organization (adapted from [11]). (C) Force-versus-extension traces generated by pulling on polyprotein containing 8 identical repeats of NuG2, a model folding domain. These records showed the characteristic "sawtooth" pattern, where the rupture of one protein domain leads to a rapid drop in force. Metal-binding pairs were engineered into the protein to stabilize the transition state. Both the apo (*grey*) and metal-bound (*black*) forms were mechanically unfolded. (D) The distribution of rupture forces for the metal-bound state (*black*) had a higher average unfolding force than the apo state (*grey*), indicating that the metal binding was disrupted in the transition state. (E) By performing this study on several residue pairs, the transition state structure can be mapped. Here, the degree of disruption of the transition state is rated from 0 (not disrupted) to 1 (fully disrupted). (A and B) reprinted from [11] and (C and D) reprinted from [37] with permissions from Elsevier.

oligomeric state and organization of Aquaporin Z (Fig. 1B) [11]. Another frontier in bio-imaging is the advent of high-speed AFM. High-speed AFM can take movies of molecular dynamics including the stepping of myosin-V along actin [24] and the response of the photosynthetic protein bacteriorhodopsin (bR) to light [25].

In imaging, lack of instrumental stability limits several exciting applications. Drift in the lateral dimensions limits the ability to return to a particular nanoscale feature. This is exacerbated when trying to return to a feature after a long delay such as when trying to re-image a feature after adding a reagent. Lateral drift also limits the signal-to-noise ratio in an image [26], since the image must be acquired too quickly to average away thermal motions of the probe, a common technique in high-resolution optical-trapping studies [27,28]. Vertical drift is also problematic. Unwanted motion in the vertical direction can result from motion of the sample relative to the AFM cantilever (position drift) or bending of the cantilever itself (force drift). Force drift is particularly problematic since the images of biological molecules can vary with force [29]. During contact mode imaging, the force set point is typically manually updated by the user to compensate for drift to maintain high-resolution imaging [30]. Hence, force drift degrades the outcome, interpretability, and user friendliness of imaging experiments.

Force spectroscopy is another way that AFM explores the world of biology by probing the folding and unfolding of proteins [1,9] and the strength of intermolecular bonds [7]. In this type of experiment, the molecule under study is stretched between the tip and the surface, typically using non-specific adhesion but increasingly with specific bonds [31–34]. The AFM tip is then retracted from the surface at a set velocity, and the force is recorded as a function of molecular extension to produce a plot such as the ones shown in Fig. 1C. By performing these mechanical experiments at a number of different pulling rates, details of the energy landscape can be derived, including the height of the unfolding barrier and the location of the transition state [35,36]. In one interesting application, Shen et al. [37] mapped the transition state structure of a protein by adding metal-binding pairs through mutagenesis and comparing force curves in the presence and absence of metal ions (Fig. 1C–E). Force spectroscopy has also probed ligand–receptor bonds from diverse systems ranging from streptavidin–biotin [35] to virus–receptor interactions [38].

Minimizing drift in the vertical (z) dimension is critical to force spectroscopy experiments. Currently, instrumental drift limits the minimum speed available to force spectroscopy experiments to approximately 5–10 nm/s on a state-of-the-art commercial AFM, and 1 nm/s under ideal conditions on a custom AFM after letting the system equilibrate overnight [39]. Ideally, pulling experiments could be slowed to the point where the tip is actually allowed to stop, and held at a constant tip-sample separation. Such stability would facilitate equilibrium studies of the folding and unfolding

of proteins and nucleic acids over long periods, similar to prior work with optical traps [40–42].

Integration of AFM with advanced spectroscopic techniques has enabled combining spatially resolved chemical identification with topography. Three promising techniques are tip-enhanced Raman scattering (TERS) [43], Raman force probe microscopy [44], and near-field infrared spectroscopy [45,46]. In TERS and other tip-based imaging modalities, the AFM tip concentrates the light to boost the optical signal so the spectrum of the molecules can be measured with ~20-nm lateral resolution [47]. To date, most experiments are done in air, but can still yield interesting biological data such as the oxidation states of different cytochrome *c* molecules in a mitochondrion [48]. Raman force probe microscopy offers enhanced lateral resolution (~3 nm) [44]. Finally, chemical probing of biological materials can be extended to bonds that have weak Raman signals, such as peptide bonds. In collaboration with Prof. Markus Raschke's group, we recently identified membrane proteins in a native lipid bilayer (purple membrane) via their Amide I vibrational mode using scattering-type scanning near-field optical microscopy (*s*-SNOM) in air (Fig. 2) [49]. Overall, all three techniques show great promise and their biological impact will be enhanced by acquiring spectroscopic information in liquid [50,51].

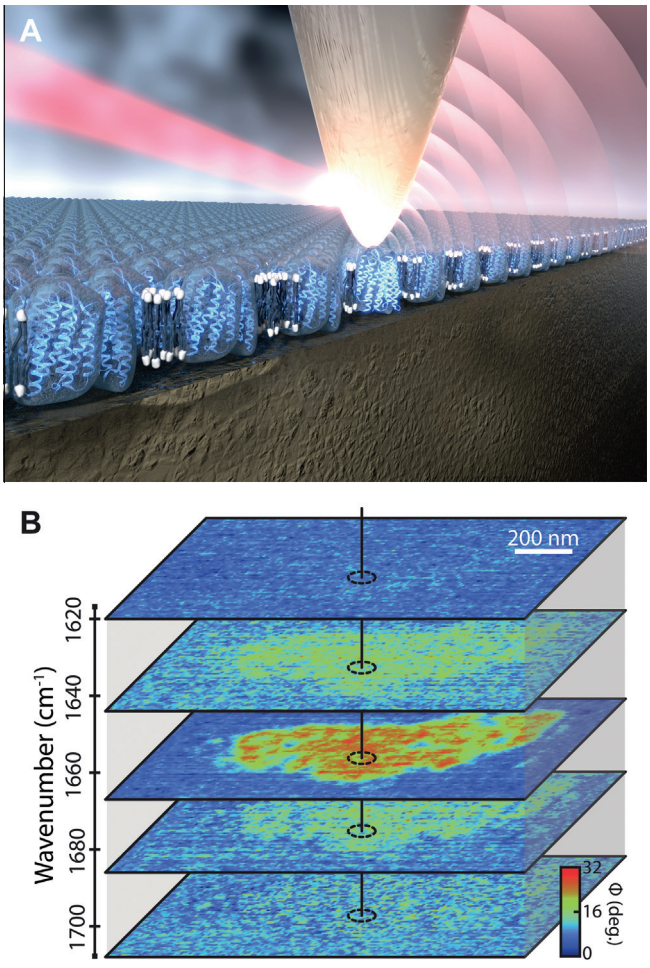

Fig. 2. Near-field IR-vibrational imaging of the membrane protein bacteriorhodopsin (bR) in its native lipid bilayer (e.g., purple membrane) produces images based on vibrational modes of the amide backbone. (A) Artist's conceptual drawing of the technique. The protein's structure (*blue*) is probed by a laser (*from left*), and the near-field scattered signal is detected. (B) Chemically specific imaging of bR's Amide I bonds with ~20-nm lateral resolution is demonstrated by varying the probe frequency around the Amide I bond's resonance (1667 cm^{-1}) in air on a gold surface. In this instrument, the AFM also simultaneously acquires a topological image (not shown). (A) Copyright 2014 B. Baxley/JILA (B) Reprinted with permission from [49]. Copyright 2013 American Chemical Society.

Like most AFM-based imaging techniques, nano-chemical imaging suffers from general tip-sample drift. This issue is exacerbated by the significant time per pixel (~10 s) necessary to acquire a spectrum [43]. Additionally, the excitation laser and the tip used to concentrate the light need to be stable relative to each other. Achieving this combined stability will help open the door to many future studies.

In summary, there are a large range of important applications of AFM limited by instrumental drift. Instrumental drift is caused by a wide range of factors that are harder to mitigate at biologically relevant conditions (in liquid at room temperature) than isolated, cryogenic conditions used to topographically map out the structure of single small molecules (Fig. 3) [52,53]. Ideally, we would like to bring the stability and precision achieved in cryogenic conditions to AFM in liquid. The challenges include Brownian motion, evaporation, temperature gradients, and acoustic noise, all of which degrade instrumental stability. AFM manufacturers have put significant effort into addressing position stability through passive means such as improved mechanical design and thermal stability. However, further reduction in lateral and vertical drift requires an active approach.

This review focuses on a set of techniques to enable an ultrastable AFM (US-AFM) for biophysical research. A number of other excellent recent reviews are available discussing techniques [6,54,55] and biological applications [3,5,13,56,57] of AFM. Over the last few years, we have developed a laser-guided AFM that achieves a 100-fold improvement in tip-sample stability [26]. As will be discussed below, this technique is the nanoscale equivalent of noise-cancelling headphones. Environmental noise is measured and actively compensated for in real time. The enhanced stability afforded by this ultrastable AFM then allowed us to uncover a significant cause of force drift in bioAFM, the gold coating on the cantilever. By removing the gold, we improved the force precision and stability of bioAFM by a factor of 10, achieving sub-pN precision [58].

To be broadly useful, we want to couple this high precision with improved throughput. One slow step is finding sparsely distributed biological structures for detailed studies. Another bottleneck is the long time (hours to overnight) that it takes for the instrument to equilibrate after loading a new sample or cantilever. The additional optics necessary for the US-AFM also facilitate optical detection of unlabeled biological structures. Such label-free imaging reduces the time to find regions of interest and preserves the physical integrity of the sample and the AFM tip [59]. Our uncoated AFM cantilevers had an additional benefit; they routinely achieved sub-pN force precision in just 30 min after mounting, even on commercial AFMs [58]. These combined techniques facilitate high-precision imaging and force spectroscopy studies.

2. Achieving positional stability: ultrastable AFM

As discussed above, tip-sample stability is a critical issue to improving AFM performance. While often discussed in the context of lateral or vertically stability, this is really a three-dimensional (3D) problem that needs a 3D solution. The most popular methods to combat lateral drift are image-tracking techniques [60,61], which compare sequential images and either computationally or through active means compensate for drift. The advent of high-speed AFM has led to more reliable tracking [62], because the drift between images is less. Interferometric stabilization is often used in high-precision physics experiments, but, in AFM applications, such stabilization requires affixing a diffraction grating to the back of the cantilever holder and the sample [63].

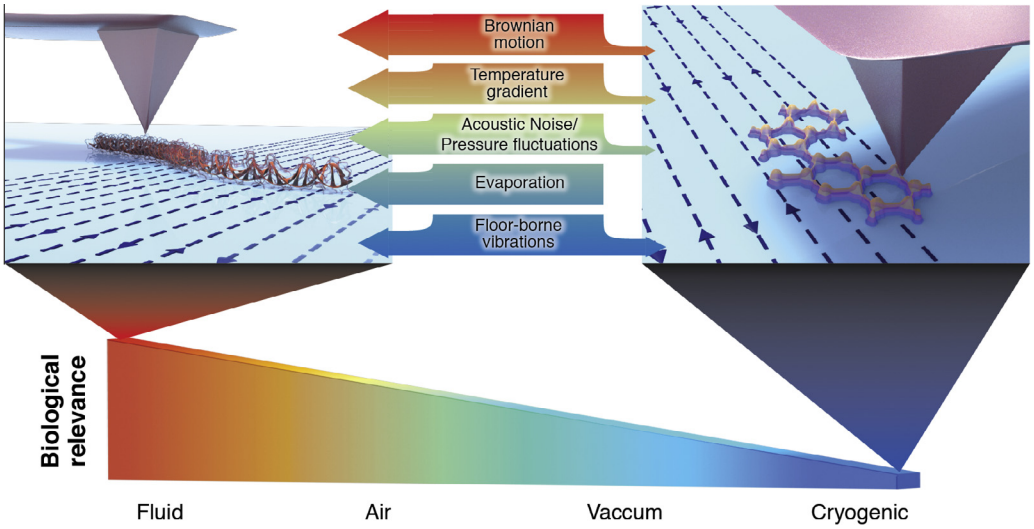

Fig. 3. AFM in biological conditions is subject to a number of perturbative sources not found in cryogenic conditions. Mitigation of these perturbations enhances the precision and stability of AFM, in general, and for biological studies, in particular.

A handful of techniques have been proposed [30,62,64] to combat vertical drift during imaging. In one innovative design [64], an AFM containing two independently steerable optical-lever-arm detection systems measured a chip containing two different length AFM cantilevers. The longer cantilever enabled vertical stabilization of the sample relative to the cantilever holder. The shorter cantilever then probed the biophysical sample. The virtue of this technique is that it uses commercially available cantilevers. However, it provides for only one axis of stabilization.

To stabilize the tip-sample separation in 3D, we adapted laser-detection techniques developed for optical traps [65] and extended them to AFM [26]. The central idea is to measure the position of the surface with one laser and the position of the AFM tip with a second laser (Fig. 4A). In this configuration, it is the differential stability between two laser beams that is critical, rather than their absolute stability. Laser-based detection of bead motion in optical traps has detected bead position in 3D with 1-Å precision [66]. To leverage this technology, we integrated these concepts into a package that was compatible with AFM [67] and effectively deconvolved the complex optical signal inherent in scattering light off of asymmetric AFM tips [68]. The combination of these advancements let us actively stabilize the tip-sample position of an AFM in 3D, originally at ambient conditions [26] and now in liquid.

To implement this stabilization, one laser beam scatters off the AFM tip, and the other laser beam scatters off a silicon post fabricated onto the glass slide. These signals are collected onto quadrant photodetectors (QPDs). A voltage change in the x direction (V_x) provides information on the x-position of the object, similarly with V_y. The total light incident on the detector V_z, often called the sum voltage, provides vertical information, though it is quite sensitive to intensity fluctuations in the detection beam [69]. The resulting set of six position measurements are then used to separately stabilize the tip and the sample using two independent 3D nanopositioning stages. The benefits of such stabilization are immediately apparent. In Fig. 4B, the sample was stabilized for 100 s after which the stabilization was turned off, resulting in substantial drift in all 3 axes. Such stabilization of the tip and the sample only yields improved tip-sample stability – the desired goal – if the two detection lasers are stable with respect to each other. Key to our success is that we achieved a differential pointing stability of 0.2 Å [67]. Excellent differential stability is achieved by minimizing the beam path and the number of non-common optical elements [67,68]. Moreover, the effects of thermal expansion are minimized by measuring the motion of the sample very close (~10 μm) to the object under study. Finally, our feedback rate (500 Hz) eliminates low-frequency drift but not the inherent Brownian motion of the cantilever.

The main challenge for controlling AFM tips is their asymmetric shape. This asymmetry leads to cross-talk: a motion in y leads to a change not only in V_y but also in V_x and V_z. A calibration associated with each new tip solves the crosstalk issue. For force spectroscopy applications, the tip is raster scanned in a 3D volume (e.g., $25 \times 25 \times 200\ \mathrm{nm}^3$), measuring V_x, V_y, and V_z at each position. A fit to this data yields a set of parameters (a_{ijk}) that precisely determined x, y, and z motion [70] from voltage data using a fourth-order polynomial of the form:

$$x(V_x, V_y, V_z) = \sum_{i,j,k=0}^{i+j+k=4} a_{ijk} V_x^i V_y^j V_z^k, \tag{1}$$

where each set of exponents i, j, k on the voltages has a unique fit coefficient a_{ijk}. The additional computational complexity is efficiently handled using field programmable gate arrays for fast deterministic feedback [68].

Our tip detection laser enables the precise measurement of the tip's position in 3D. Thus, we can independently measure the conjugate variables for force and extension. Specifically, we can both detect and, thereby, control tip position in 3D with 0.3-Å precision and stability in a useful bandwidth (Δf = 0.01–10 Hz) for biological assays. Control of the AFM tip when it is off of the surface enables a new mode of single molecule force spectroscopy (SMFS), an extension clamp. The benefits of such an extension clamp have recently been described from a theoretical point of view [71]. Three-dimensional detection of the tip also yields insight into the 3D forces acting on a cantilever during tapping-mode imaging [72].

Our ultrastable AFM requires substrates with a scattering feature to track sample motion. A simple way to make this feature is to melt glass beads onto the surface. This allows for stabilization to ~1 nm, because these beads move relative to the surface on a sub-nm level [69]. Improved stability requires a reference mark that is firmly attached to the surface. We currently use an array of silicon posts (~800-nm dia., 50-nm tall [67]) that are fabricated onto a cover slip using a shadow mask, a thin membrane with holes in it. There are a number of ways to make these masks from

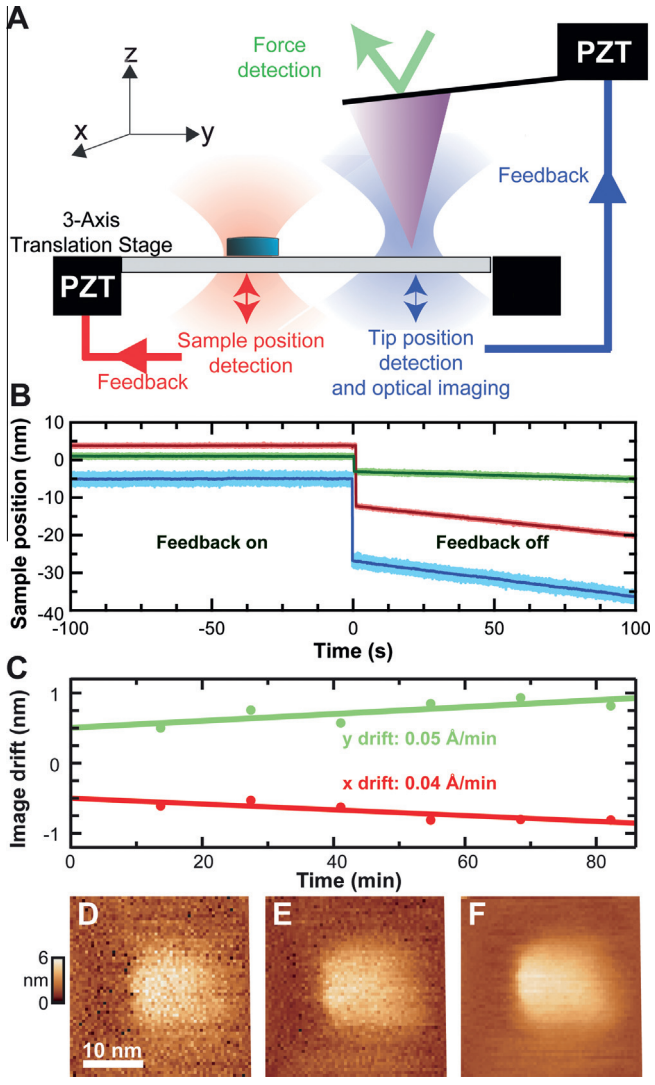

Fig. 4. Laser-guided atomic force microscopy. (A) Schematic of the ultrastable AFM showing three lasers. The traditional cantilever deflection detection laser (*green*) measures force. Two additional lasers (*red* and *blue*) measure the sample and tip positions relative to their respective laser foci. These measurements are then used in feedback loops to two separate 3-axis translation stages (PZT) to stabilize the sample and the AFM tip. The tip-detection laser is also used for optical imaging. (B) Position-versus time record during and after activation sample stabilization. In this assay, one laser was used to stabilize the sample, and the other to record its position in x (*red*), y (*green*), and z (*blue*). This "out of loop" stability was 0.3 Å in x and y, and 0.7 Å in z ($\Delta f = 0.01$–10 Hz). Stabilization was turned off at $t = 0$, and the sample drifted at its inherent rate. (C) Measured residual drift rates during active stabilization deduced from a series of sequential images show drift rates of 0.04 and 0.05 Å/min in x and y, respectively. (D–F) Sequential images of a 5-nm gold nanosphere taken with increased averaging time per pixel. Specifically, the averaging time per pixel was 0.2, 2, and 20 ms for panels D–F, respectively. Panels (C–F) reprinted with permission from [26]. Copyright 2009 American Chemical Society.

X-ray windows (Silson), including using an electron-beam resist [69], making the holes with a focused-ion-beam mill, and purchasing windows with holes already in place (DuraSiN Mesh, Protochips). The needed glass cover slips with fiducial marks are relatively simple to make with standard clean room equipment (e.g., an e-beam evaporator) and a process carried out by undergraduates in our lab.

The ultimate test of lateral instrument stability over long-time scales is imaging, since it convolves both tip and sample motion. To demonstrate the stability of the US-AFM, we imaged a 5-nm gold bead over an extended period (>1 h). Visual inspection showed a stationary image. To quantify the residual motion, we cross-correlated the first image with each subsequent image, and reported the position of the peak (Fig. 4C). The residual drift was a mere 0.04 and 0.05 Å/min in x and y [26], a 100-fold improvement over prior state of the art at ambient conditions [73] and similar to drift rates at cryogenic temperatures [74].

One of the early goals of the US-AFM project was to improve an image's signal-to-noise ratio by averaging the Brownian motion of the cantilever [26]. Such averaging is widely used in optical-trapping studies, but not in AFM due to tip-sample drift. The Å-scale tip-sample stability of the US-AFM allowed us to slow down scanning and thereby demonstrate a 5-fold improvement in the signal-to-noise ratio (Fig. 4D–F).

3. A fringe benefit: rapid localization of biological structures

A time-consuming step in AFM is often finding the region of interest you want to study. Many interesting biological structures are optically transparent and small. Thus, they are not resolved in standard optical microscopy found on commercial AFMs. Fluorescence microscopy is an option, but requires labeling the molecules, an added step that can potentially inhibit functionality. Therefore, a label-free detection technique is desirable. Recently, tiny variations in back-scattered light were used to detect small structures such as viruses and microtubules [75,76]. The optics used for that imaging is a subset of what is needed for the US-AFM, allowing us to integrate label-free back-scattered imaging with the US-AFM. Indeed, the combination of a tightly focused laser beam and low-noise electronics developed for the US-AFM enabled us to detect 5-nm tall patches of membrane protein with a high signal-to-noise ratio (~20) [59]. To achieve this sensitivity requires a very stable laser. Our intensity variations were 1 part in 50,000 over a broad frequency range ($\Delta f = 0.02$–100 Hz). We imaged by raster scanning the sample through the stationary tip-detection laser when the tip is retracted from the surface (Fig. 5A). A structure of interest is located in this image and then aligned with the detection laser. The AFM tip, which is aligned to the same laser, can then be deterministically brought down onto that structure (Fig. 5B).

This label-free detection technique goes a long way towards solving the "needle in the haystack" problem for finding sparsely distributed biological structures. Very large areas (>30 × 30 μm^2) can be scanned optically (Fig. 5C). Interesting features can be selected (Fig. 5C, box) and scanned in detail (Fig. 5D). As shown in Fig. 5E, the resulting AFM image is aligned with the optical image, allowing the tip to be engaged only with the object of interest. We find this optical scanning preserves the sharpness and cleanliness of the tip by avoiding large-area scans and collisions between the tip and larger biological aggregates (Fig. 5C, arrow). Another positive feature is that this scanning can be done during the first 30 min after mounting a sample, a time usually lost in AFM as the instrument equilibrates. Indeed, optical scanning is so simple that we find it a useful technique for evaluating sample preparation techniques.

4. Improving force precision

Single-molecule studies of macromolecular folding are having an impact on increasingly complex biological structures, from RNA to proteins [77–80]. Force-induced unfolding is proving particularly insightful, since the application of force tilts the folding energy landscape in a controlled and quantifiable manner that can be theoretically modeled [36]. An exciting class of experiments, called equilibrium studies, are ones in which the molecule repeatedly folds and unfolds. The observed folding kinetics are

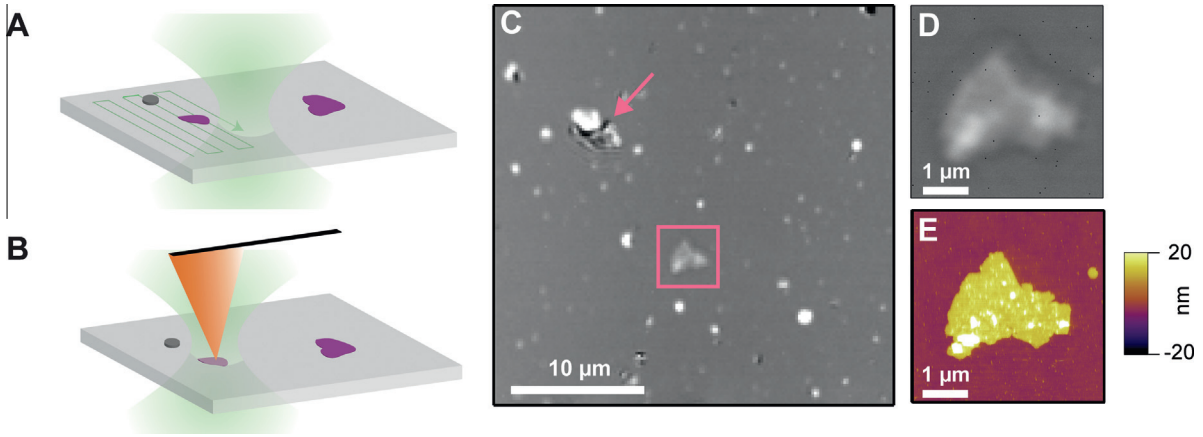

Fig. 5. Label-free optical imaging of AFM samples to locate regions of interest and minimize tip and sample degradation. (A) Schematic of the assay showing a sample containing patches of purple membrane raster scanned through a focused laser beam. The back-scattered light is collected and used to generate an image. In this cartoon, the grey circle represents the silicon post, and the purple shapes are patches of purple membrane that contain bacteriorhodopsin. (B) A membrane patch is aligned to the laser. The AFM tip is aligned to the same laser, positioning the AFM directly above the region of interest without having to scan the sample with the AFM tip. (C) A label-free optical image of a purple membrane in liquid generated as in (A) show several features, such as a membrane patch (pink box) and a large object to be avoided (pink arrow). (D) A more detailed optical image of a purple membrane patch. (E) AFM image of same region as in (D) demonstrates excellent (40 nm) registration between optical and AFM images. Reprinted from [59].

sensitive to sub-pN changes in force [81]. However, the force precision of AFM is typically 5–10 pN, which hinders the application of AFM to these studies. Force drift not only alters the dynamics between the start and end of the record, it also obscures identification of states in this class of equilibrium folding/unfolding studies. Hence, force stability over the full duration of the experiment is much more important than force precision in a narrow-bandwidth and also more difficult to achieve.

Initially, we expected that the long-term force stability in AFM would be solved by using our US-AFM. Preliminary data with the US-AFM showed that position stability was only half the problem: force drift remains. Specifically, we held a molecule under constant extension, but observed long-term drift in the measured force. Molecules, like rubber bands, should not exhibit a change in force under constant extension (assuming no refolding). We ultimately traced the source of this drift to the AFM cantilever itself. Its zero-force position was changing as a function of time, drifting hundreds of nanometers over an hour [58]. In many experiments, this drift would be unobserved. However, our ability to clamp extension over long periods allowed us to unambiguously identify and reduce drift in the zero-force position of a cantilever.

By removing a cantilever's gold coating, we reduced the cantilever's drift and, thereby, improved force precision and stability (Fig. 6A) [58]. It has long been known that cantilevers coated on only one side drift due to thermal effects [82]. However, we observed comparable drift even when using fully coated cantilevers in a temperature-controlled AFM. For these fully coated cantilevers, removing the gold coating led to a ~10-fold reduction in drift over 3 h [900 vs 70 nm (RMS, $N = 10$)].

Traditionally, the gold coating on the cantilever is thought to be critical for high-precision measurement since the gold enhances the reflectivity off of these very thin (170 nm) cantilevers. Enhanced reflectivity, in turn, improves the sensitivity of the optical lever arm. Unexpectedly, we showed that for these uncoated soft (spring constant $k \approx 6$ pN/nm) cantilevers there was no loss in positional precision at short-time scales (1 ms) despite a significant loss in sensitivity. A good metric for testing force stability over the duration of the experiment is the integrated force noise. We achieved an integrated force noise of 0.5 pN over a broadly useful bandwidth ($\Delta f = 0.01$–10 Hz), a 10-fold improvement over gold-coated cantilevers [58] (Fig. 6A).

Many AFM users can immediately benefit from these improvements in force stability and precision. While the US-AFM was critical in uncovering the adverse effects of gold coating, the benefits of using uncoated cantilevers are not limited to US-AFM. We achieved similar sub-pN precision using a commercial cantilever on a commercial instrument (Cypher, Asylum Research). Operationally, it is very easy to remove the gold (and the underlying chromium layer). It takes only two short (30-s) chemical etches using commercial gold and chromium etchant (Transene type TFA and 1020, respectively) according to manufacturer instructions. The cantilevers are then rinsed in deionized water and dipped in isopropanol. Importantly, this sub-pN stability over 100 s is not rare. Rather, a majority of the cantilevers tested achieved this force precision just 30 min after mounting. Indeed our worst uncoated cantilever's force stability was 2.5-fold better than our best gold-coated cantilever. An added benefit is that users no longer have to wait hours for an AFM to settle.

Force stability benefits not only force spectroscopy experiments, but also imaging applications. Different imaging forces lead to changes in the characteristic lattice of bacteriorhodopsin [29]. Unfortunately, even during "constant" force imaging, variations in force arise due to drift in the cantilever's zero-force position. As a result, the sub-structure of the bR lattice varied while imaging with a gold-coated cantilever (Fig. 6B and C) [83]. Thus, while the goal is constant force imaging, the force is not truly constant. Indeed, the variation in force is so large during image acquisition that the user must continually adjust the AFM to keep the tip in contact with the sample. In contrast, by using uncoated cantilevers, the resulting images showed essentially no distortion over long periods (Fig. 6D and E). Furthermore, the set point remains essentially constant, reducing the need for manual adjustments by the user (Fig. 6F) [83].

5. Cantilever selection for high-precision AFM

The traditional view in AFM is that shorter cantilevers lead to better force precision due to decreased hydrodynamic drag (β) [84]. This improvement is a consequence of the fluctuation–dissipation theorem $\Delta F = \sqrt{4k_B T \Delta f \beta}$, where ΔF is the force precision, $k_B T$ is the thermal energy, and Δf is the bandwidth of the measurement. This result assumes the measured motion of the cantilever is

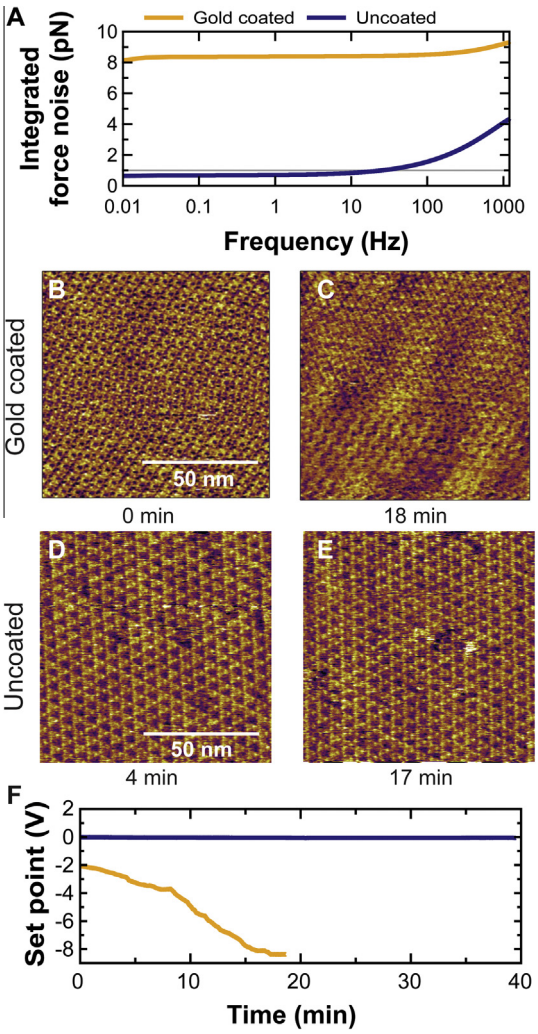

Fig. 6. Uncoated cantilevers benefit both force spectroscopy and imaging applications on a commercial AFM. (A) Integrated force noise, a measure of force stability, plotted as a function of frequency for coated (*gold*) and uncoated (*blue*) long Biolevers. The uncoated cantilever shows a ~10-fold improvement relative to the coated cantilever, achieving a force precision of 1 pN (*grey line*) over a broad frequency range (Δf = 0.01–25 Hz). (B and C) Images of bacteriorhodopsin lattice taken with a gold-coated Biolever Mini at 0 and 18 min shows significant variation in the lattice appearance due to force drift. While these images were taken in contact mode at constant force, the set point of the AFM had to be manually updated to keep the tip on the surface, another indication of force drift. (D and E) Similar images taken with an uncoated cantilever at 4 and 17 min show minimal change in the lattice structure and also required minimal manual adjustment to the set point. With the gold-coated cantilever, the user must constantly adjust the setpoint to maintain suitable imaging conditions, which is not necessary with an uncoated cantilever. (F) Plot of user-adjusted setpoint as a function of time while using gold-coated (*gold*) and uncoated (*blue*) cantilevers. Panel A reprinted with permission from [58]. Copyright 2012 American Chemical Society. B–F reprinted from [83] with permission from Elsevier.

limited by thermal motion. However, when using gold-coated cantilevers intended for high-precision force spectroscopy applications, this assumption breaks down at surprisingly short time scales (~1 ms) due to a fixed amount of positional noise (Δx) in the optical lever arm [83]. This positional noise adversely affects force precision (ΔF) more with stiffer cantilevers than with soft ones. In summary, short-term force precision is improved by lowering β. Long-term force stability is achieved by lowering k.

Hence, the optimum choice of a cantilever depends on the duration of the experiment. A specific example helps clarify this compromise. Two commonly used cantilevers are the long BioLever (L = 100 μm; k = 7 pN/nm) and BioLever Mini (L = 40 μm; k = 100 pN/nm), both from Olympus. Recent data from our lab shows that the longer cantilever has better force precision than the shorter cantilever at 25 ms for uncoated cantilevers [58] with the crossover for gold coated cantilevers occurring at even shorter times scales (10 ms). To put this time in perspective, mechanically unfolding a polyprotein, a common substrate for AFM-based single molecule force spectroscopy [85], takes ~400 ms at a typical velocity (500 nm/s). Hence, minimizing drift in AFM cantilevers [58], originally motivated by equilibrium studies of protein folding, can improve SMFS assays that are typically thought to be unaffected by drift. Micromachining of commercial cantilevers [86,87] can avoid this tradeoff between short-term force precision and long-term force stability by achieving a 10-fold reduction in both β and k, leading to additional enhancements in SMFS [88].

6. Prospects for ultrastable AFM in biophysics

Currently, the US-AFM provides a ~100-fold improvement in tip-sample positional stability but it is technically demanding (see below). A wide range of AFM applications can benefit from this enhanced stability, including biophysical assays that were previously inaccessible or very hard to reproduce due to instrumental limitations, such as hovering a tip over a protein to measure enzymatically induced conformational fluctuations [89].

Chemically sensitive imaging of materials with nanometer-scale resolution is also enhanced by improved AFM stability. In recent work, Yano et al. [90] created an actively stabilized TERS instrument, where the same beam was used for both TERS imaging and optical stabilization. As a result, they held the tip position stable relative to the excitation beam for 40 min. Future work can integrate tip-sample stabilization for TERS and other tip-based infrared spectroscopy [45,49] in biophysical assays.

A frontier in bioAFM is probing live cells [91,92] but such studies are challenging [93]. A hallmark of life is motion. Structures inside of the cell grow, shrink, and move. Moreover, cells move relative to the underlying substrate. While, in general, we discuss the improvements afforded by the US-AFM in the context of tip-sample stability, more technically, it is tip-substrate stability. Thus, the Ångstrom-level substrate stability will not immediately translate to similar sample stability in cellular studies. Nonetheless, improved substrate stability can still be useful, particularly at physiologically relevant elevated temperature (37 °C) where temperature-induced drift may be exacerbated. In one example, Fuhs et al. [94] wanted to measure the growth of neurons on hour time scales at 37 °C, but *substrate* drift hindered such experiments. They solved this problem by integrating optical-based stabilization into a modified commercial AFM. Since this cellular study required nanometer-scale, not Ångstrom-scale, stabilities, they used glass beads stuck to the cover slip as positional fiducial marks, an easy-to-make substrate. Achieving nanometer or even Ångstrom-scale *sample* stability is significantly more challenging. While adding a reference mark, such as a large gold bead via immuno-gold staining, to the surface of a cell is possible, the key issue will be time-dependent variations in the index of refraction within the cell. These variations will alter the beam profile of a laser passing through the cell and be interpreted as sample motion to be corrected in our stabilization technique.

For in vitro studies, two current issues limit the broader adoption of the US-AFM. First, it is not straightforward to combine US-AFM with a birefringent substrate, such as calcite or mica, the preferred substrate for high-resolution imaging. Birefringence interferes with our laser-based stabilization technique, since the laser beams pass through the sample substrate. A path forward is to integrate a thin layer of mica on glass with fiducial marks. This

should minimize the adverse effect of mica and thus enhance the utility of the US-AFM for bio-imaging. Second, US-AFM requires separate and independent control of the tip and the sample, which is not available in current commercial AFMs. Therefore, a potential user must build a custom AFM incorporating two independent three axis stages [26] and a pair of actively stabilized lasers [67,69]. As the mica issue is resolved and demand for ultrastable AFM capabilities grows, we see no fundamental barrier to commercialization. Unlike small-format commercial AFMs optimized for stability [e.g., Cypher (Asylum Research)], the US-AFM is built upon an inverted microscope so integration with fluorescence imaging is straight forward.

7. Conclusions

Atomic force microscopy is a powerful technique for studying the structure, dynamics, and energetics of biological systems in their native environment. Despite the challenges of performing high-precision measurements in liquid at room temperature, AFM can image membrane proteins with sub-nm lateral resolution and mechanically manipulate molecules with sub-pN force precision. AFM's usefulness is improved by extending and improving upon these already impressive capabilities over an ever-widening range of time scales. High-speed AFM is one important direction in the field. On the other end of the spectrum, enhancements in stability enable a wide range of experiments, including measuring proteins fold and unfold hundreds to thousands of times at equilibrium conditions.

Historically, AFM helped pioneer the mechanical unfolding of single proteins [1,2,85,95]. Most of these early studies used rapid-stretching protocols (50–5000 nm/s), in part, to minimize the effects of drift. These non-equilibrium studies yielded a relatively small number of transitions per molecule under rapidly varying load. In the past decade, equilibrium experiments with optical traps have had a growing impact, particularly since the adoption of the dual-trap assay [96] in such studies [40,97,98]. The main advantage of optical traps over AFM is their better short-term force precision coupled with long-term stability in both position and force.

Our recent work has focused on bringing the benefits of optical trapping to AFM to open up a range of new single-molecule AFM experiments, particularly enhanced-equilibrium studies of proteins. AFM offers a number of advantages over optical trapping. Highly stable, user-friendly instruments are commercially available from a number of vendors. Additionally, AFM is inherently a surface-based technique, allowing for a broader range of systems to be studied than in a dual-beam optical-trapping assay. For example, the small surface area of an AFM tip facilitates extracting an individual membrane protein from a lipid bilayer for folding, and unfolding studies [2] and, on a more technical level, AFM is compatible with shorter and therefore stiffer, linkages to the force probe for improved sensitivity. Moreover, it avoids the use of high-powered lasers and the associated potential for radiation-induced damage.

In the last 5 years, we have made significant progress towards bringing the stability and precisions of optical traps to AFM. Specifically, we developed the ability to track and control the position of an AFM tip to 0.3 Å in 3D using laser-based detection techniques adopted from optical-trapping studies [26]. The resulting atomic-scale tip-sample control, previously restricted to cryogenic temperatures and ultrahigh vacuum, is now available to a wide range of perturbative operating environments.

Initial applications of this US-AFM to force spectroscopy uncovered another major source of instrumental limitation in AFM: force drift. By removing a cantilever's gold coating, we extended AFM's typical force precision of ~5–10 pN down into the 0.5 pN regime over a broad bandwidth (Δf = 0.01–10 Hz). One of the unexpected results from this study was that deflection measurements of soft cantilevers on short times (1 ms) were not adversely affected by the 10-fold loss in optical signal due to removing the gold. A broad range of single-molecule studies can immediately benefit from using gold-free cantilevers. Sub-pN force sensitivity, which has traditionally been associated with optical traps and magnetic tweezers [99,100], is now routinely accessible with a commercial AFM in liquid using a simple modification to popular commercial cantilevers. We hope these accessible advances, along with the more technically demanding US-AFM, will facilitate a new generation of more precise AFM-based biophysical studies.

Acknowledgements

We thank Brad Baxley for scientific illustration and members of the Perkins group for careful reading of this manuscript. This work was supported by the National Science Foundation [DBI-0923544, Phys-1125844], and National Institute of Standards and Technology – United States. Mention of commercial products is for information only; it does not imply NIST's recommendation or endorsement. TTP is a staff member of NIST's Quantum Physics Division.

TTP is a co-inventor on two patents related to Ångström-scale stabilization. These patents are assigned to the US Government.

References

[1] Rief, M., Gautel, M., Oesterhelt, F., Fernandez, J.M. and Gaub, H.E. (1997) Reversible unfolding of individual titin immunoglobulin domains by AFM. Science 276, 1109–1112.
[2] Oesterhelt, F., Oesterhelt, D., Pfeiffer, M., Engel, A., Gaub, H.E. and Muller, D.J. (2000) Unfolding pathways of individual bacteriorhodopsins. Science 288, 143–146.
[3] Muller, D.J. and Dufrene, Y.F. (2008) Atomic force microscopy as a multifunctional molecular toolbox in nanobiotechnology. Nat. Nanotechnol. 3, 261–269.
[4] Puchner, E.M. and Gaub, H.E. (2012) Single-molecule mechanoenzymatics. Annu. Rev. Biophys. 41, 497–518.
[5] Muller, D.J. and Dufrene, Y.F. (2011) Atomic force microscopy: a nanoscopic window on the cell surface. Trends Cell Biol. 21, 461–469.
[6] Ando, T. (2012) High-speed atomic force microscopy coming of age. Nanotechnology 23, 062001.
[7] Florin, E.-L., Moy, V.T. and Gaub, H.E. (1994) Adhesion forces between individual ligand–receptor pairs. Science 264, 415–417.
[8] Puchner, E.M. and Gaub, H.E. (2009) Force and function: probing proteins with AFM-based force spectroscopy. Curr. Opin. Struct. Biol. 19, 605–614.
[9] Fernandez, J.M. and Li, H. (2004) Force-clamp spectroscopy monitors the folding trajectory of a single protein. Science 303, 1674–1678.
[10] Bippes, C.A., Zeltina, A., Casagrande, F., Ratera, M., Palacin, M., Muller, D.J. and Fotiadis, D. (2009) Substrate binding tunes conformational flexibility and kinetic stability of an amino acid antiporter. J. Biol. Chem. 284, 18651–18663.
[11] Trinh, M.-H. et al. (2012) Computational reconstruction of multidomain proteins using atomic force microscopy data. Structure 20, 113–120.
[12] Drake, B. et al. (1989) Imaging crystals, polymers, and processes in water with the atomic force microscope. Science 243, 1586–1589.
[13] Casuso, I., Rico, F. and Scheuring, S. (2011) Biological AFM: where we come from – where we are – where we may go. J. Mol. Recognit. 24, 406–413.
[14] Binnig, G., Quate, C.F. and Gerber, C. (1986) Atomic force microscope. Phys. Rev. Lett. 56, 930–933.
[15] Meyer, G. and Amer, N.M. (1988) Novel optical approach to atomic force microscopy. Appl. Phys. Lett. 53, 1045–1047.
[16] Leung, C. et al. (2012) Atomic force microscopy with nano-scale cantilevers resolves different structural conformations of the DNA double helix. Nano Lett. 12, 3846–3850.
[17] Zhong, Q., Inniss, D., Kjoller, K. and Elings, V. (1993) Fractured polymer/silica fiber surface studied by tapping mode atomic force microscopy. Surf. Sci. Lett. 290, L688–L692.
[18] Hansma, P.K. et al. (1994) Tapping mode atomic-force microscopy in liquids. Appl. Phys. Lett. 64, 1738–1740.
[19] Cleveland, J., Anczykowski, B., Schmid, A. and Elings, V. (1998) Energy dissipation in tapping-mode atomic force microscopy. Appl. Phys. Lett. 72, 2613–2615.
[20] Giessibl, F.J. (2001) A direct method to calculate tip sample forces from frequency shifts in frequency-modulation atomic force microscopy. Appl. Phys. Lett. 78, 123–125.

[21] Killgore, J.P., Kelly, J.Y., Stafford, C.M., Fasolka, M.J. and Hurley, D.C. (2011) Quantitative subsurface contact resonance force microscopy of model polymer nanocomposites. Nanotechnology 22, 175706.
[22] Scheuring, S., Ringler, P., Borgnia, M., Stahlberg, H., Muller, D.J., Agre, P. and Engel, A. (1999) High resolution AFM topographs of the *Escherichia coli* water channel aquaporin Z. EMBO J. 18, 4981–4987.
[23] Chaves, R.C., Teulon, J.M., Odorico, M., Parot, P., Chen, S.W.W. and Pellequer, J.L. (2013) Conformational dynamics of individual antibodies using computational docking and AFM. J. Mol. Recognit. 26, 596–604.
[24] Kodera, N., Yamamoto, D., Ishikawa, R. and Ando, T. (2010) Video imaging of walking myosin V by high-speed atomic force microscopy. Nature 468, 72–76.
[25] Shibata, M., Uchihashi, T., Yamashita, H., Kandori, H. and Ando, T. (2011) Structural changes in bacteriorhodopsin in response to alternate illumination observed by high speed atomic force microscopy. Angew. Chem. 123, 4502–4505.
[26] King, G.M., Carter, A.R., Churnside, A.B., Eberle, L.S. and Perkins, T.T. (2009) Ultrastable atomic force microscopy: atomic-scale lateral stability and registration in ambient conditions. Nano Lett. 9, 1451–1456.
[27] Abbondanzieri, E.A., Greenleaf, W.J., Shaevitz, J.W., Landick, R. and Block, S.M. (2005) Direct observation of base-pair stepping by RNA polymerase. Nature 438, 460–465.
[28] Perkins, T.T. (2009) Optical traps for single molecule biophysics: a primer. Laser Photon. Rev. 3, 203–220.
[29] Muller, D.J., Buldt, G. and Engel, A. (1995) Force-induced conformational change of bacteriorhodopsin. J. Mol. Biol. 249, 239–243.
[30] Casuso, I. and Scheuring, S. (2010) Automated setpoint adjustment for biological contact mode atomic force microscopy imaging. Nanotechnology 21, 035104.
[31] Zimmermann, J.L., Nicolaus, T., Neuert, G. and Blank, K. (2010) Thiol-based, site-specific and covalent immobilization of biomolecules for single-molecule experiments. Nat. Protoc. 5, 975–985.
[32] Taniguchi, Y. and Kawakami, M. (2010) Application of HaloTag protein to covalent immobilization of recombinant proteins for single molecule force spectroscopy. Langmuir 26, 10433–10436.
[33] Zakeri, B., Fierer, J.O., Celik, E., Chittock, E.C., Schwarz-Linek, U., Moy, V.T. and Howarth, M. (2012) Peptide tag forming a rapid covalent bond to a protein, through engineering a bacterial adhesin. Proc. Natl. Acad. Sci. U.S.A. 109, E690–E697.
[34] Popa, I., Berkovich, R., Alegre-Cebollada, J., Badilla, C.L., Rivas-Pardo, J.A., Taniguchi, Y., Kawakami, M. and Fernandez, J.M. (2013) Nanomechanics of HaloTag tethers. J. Am. Chem. Soc. 135, 12762–12771.
[35] Merkel, R., Nassoy, P., Leung, A., Ritchie, K. and Evans, E. (1999) Energy landscapes of receptor–ligand bonds explored with dynamic force spectroscopy. Nature 397, 50–53.
[36] Dudko, O.K., Hummer, G. and Szabo, A. (2008) Theory, analysis, and interpretation of single-molecule force spectroscopy experiments. Proc. Natl. Acad. Sci. U.S.A. 105, 15755–15760.
[37] Shen, T., Cao, Y., Zhuang, S. and Li, H. (2012) Engineered bi-histidine metal chelation sites map the structure of the mechanical unfolding transition state of an elastomeric protein domain GB1. Biophys. J. 103, 807–816.
[38] Rankl, C., Kienberger, F., Wildling, L., Wruss, J., Gruber, H.J., Blaas, D. and Hinterdorfer, P. (2008) Multiple receptors involved in human rhinovirus attachment to live cells. Proc. Natl. Acad. Sci. U.S.A. 105, 17778–17783.
[39] Junker, J.P., Ziegler, F. and Rief, M. (2009) Ligand-dependent equilibrium fluctuations of single calmodulin molecules. Science 323, 633–637.
[40] Stigler, J., Ziegler, F., Gieseke, A., Gebhardt, J.C.M. and Rief, M. (2011) The complex folding network of single calmodulin molecules. Science 334, 512–516.
[41] Cecconi, C., Shank, E.A., Bustamante, C. and Marqusee, S. (2005) Direct observation of the three-state folding of a single protein molecule. Science 309, 2057–2060.
[42] Woodside, M.T., Anthony, P.C., Behnke-Parks, W.M., Larizadeh, K., Herschlag, D. and Block, S.M. (2006) Direct measurement of the full, sequence-dependent folding landscape of a nucleic acid. Science 314, 1001–1004.
[43] Deckert-Gaudig, T., Bohme, R., Freier, E., Sebesta, A., Merkendorf, T., Popp, J., Gerwert, K. and Deckert, V. (2012) Nanoscale distinction of membrane patches – a TERS study of *Halobacterium salinarum*. J. Biophoton. 5, 582–591.
[44] Rajapaksa, I. and Wickramasinghe, H.K. (2011) Raman spectroscopy and microscopy based on mechanical force detection. Appl. Phys. Lett. 99, 161103.
[45] Taubner, T., Hillenbrand, R. and Keilmann, F. (2004) Nanoscale polymer recognition by spectral signature in scattering infrared near-field microscopy. Appl. Phys. Lett. 85, 5064–5066.
[46] Raschke, M.B., Molina, L., Elsaesser, T., Kim, D.H., Knoll, W. and Hinrichs, K. (2005) Apertureless near-field vibrational imaging of block-copolymer nanostructures with ultrahigh spatial resolution. ChemPhysChem 6, 2197–2203.
[47] Deckert-Gaudig, T. and Deckert, V. (2011) Nanoscale structural analysis using tip-enhanced Raman spectroscopy. Curr. Opin. Chem. Biol. 15, 719–724.
[48] Bohme, R., Mkandawire, M., Krause-Buchholz, U., Rosch, P., Rodel, G., Popp, J. and Deckert, V. (2011) Characterizing cytochrome c states – TERS studies of whole mitochondria. Chem. Commun. 47, 11453–11455.
[49] Berweger, S., Nguyen, D.M., Muller, E.A., Bechtel, H.A., Perkins, T.T. and Raschke, M.B. (2013) Nano-chemical infrared imaging of membrane proteins in lipid bilayers. J. Am. Chem. Soc. 135, 18292–18295.
[50] Schmid, T., Yeo, B.S., Leong, G., Stadler, J. and Zenobi, R. (2009) Performing tip-enhanced Raman spectroscopy in liquids. J. Raman Spectrosc. 40, 1392–1399.
[51] Opilik, L., Bauer, T., Schmid, T., Stadler, J. and Zenobi, R. (2011) Nanoscale chemical imaging of segregated lipid domains using tip-enhanced Raman spectroscopy. Phys. Chem. Chem. Phys. 13, 9978–9981.
[52] Gross, L., Mohn, F., Moll, N., Liljeroth, P. and Meyer, G. (2009) The chemical structure of a molecule resolved by atomic force microscopy. Science 325, 1110–1114.
[53] Gross, L., Mohn, F., Moll, N., Meyer, G., Ebel, R., Abdel-Mageed, W.M. and Jaspars, M. (2010) Organic structure determination using atomic-resolution scanning probe microscopy. Nat. Chem. 2, 821–825.
[54] Gan, Y. (2009) Atomic and subnanometer resolution in ambient conditions by atomic force microscopy. Surf. Sci. Rep. 64, 99–121.
[55] Flores, S.M. and Toca-Herrera, J.L. (2009) The new future of scanning probe microscopy: combining atomic force microscopy with other surface-sensitive techniques, optical and microscopy fluorescence techniques. Nanoscale 1, 40–49.
[56] Mateu, M.G. (2012) Mechanical properties of viruses analyzed by atomic force microscopy: a virological perspective. Virus Res. 168, 1–22.
[57] Alessandrini, A. and Facci, P. (2011) Unraveling lipid/protein interaction in model lipid bilayers by Atomic Force Microscopy. J. Mol. Recognit. 24, 387–396.
[58] Churnside, A.B., Sullan, R.M., Nguyen, D.M., Case, S.O., Bull, M.S., King, G.M. and Perkins, T.T. (2012) Routine and timely sub-picoNewton force stability and precision for biological applications of atomic force microscopy. Nano Lett. 12, 3557–3561.
[59] Churnside, A.B., King, G.M. and Perkins, T.T. (2010) Label-free optical imaging of membrane patches for atomic force microscopy. Opt. Express 18, 23924–23932.
[60] Abe, M., Sugimoto, Y., Namikawa, T., Morita, K., Oyabu, N. and Morita, S. (2007) Drift-compensated data acquisition performed at room temperature with frequency modulation atomic force microscopy. Appl. Phys. Lett. 90, 203103.
[61] Woodward, J.T. and Schwartz, D.K. (1998) Removing drift from scanning probe microscope images of periodic samples. J. Vac. Sci. Technol. B 16, 51–53.
[62] Husain, M., Boudier, T., Paul-Gilloteaux, P., Casuso, I. and Scheuring, S. (2012) Software for drift compensation, particle tracking and particle analysis of high-speed atomic force microscopy image series. J. Mol. Recognit. 25, 292–298.
[63] Moon, E.E., Kupec, J., Mondol, M.K., Smith, H.I. and Berggren, K.K. (2007) Atomic-force lithography with interferometric tip-to-substrate position metrology. J. Vac. Sci. Technol. B 25, 2284–2287.
[64] Choy, J.L., Parekh, S.H., Chaudhuri, O., Liu, A.P., Bustamante, C., Footer, M.J., Theriot, J.A. and Fletcher, D.A. (2007) Differential force microscope for long time-scale biophysical measurements. Rev. Sci. Instrum. 78, 043711.
[65] Visscher, K., Gross, S.P. and Block, S.M. (1996) Construction of multiple-beam optical traps with nanometer-resolution position sensing. IEEE J. Sel. Top. Quant. Electron. 2, 1066–1076.
[66] Pralle, A., Prummer, M., Florin, E.-L., Stelzer, E.H.K. and Horber, J.K.H. (1999) Three-dimensional high-resolution particle tracking for optical tweezers by forward scattered light. Microsc. Res. Tech. 44, 378–386.
[67] Carter, A.R., King, G.M. and Perkins, T.T. (2007) Back-scattered detection provides atomic-scale localization precision, stability, and registration in 3D. Opt. Express 15, 13434–13445.
[68] Churnside, A.B., King, G.M., Carter, A.R. and Perkins, T.T. (2008) Improved performance of an ultrastable measurement platform using a field-programmable gate array for real-time deterministic control. Proc. SPIE 7042, 704205.
[69] Carter, A.R., King, G.M., Ulrich, T.A., Halsey, W., Alchenberger, D. and Perkins, T.T. (2007) Stabilization of an optical microscope to 0.1 nm in three dimensions. Appl. Opt. 46, 421–427.
[70] Lang, M.J., Asbury, C.L., Shaevitz, J.W. and Block, S.M. (2002) An automated two-dimensional optical force clamp for single molecule studies. Biophys. J. 83, 491–501.
[71] Suzuki, Y. and Dudko, O.K. (2013) Single molecules in an extension clamp: extracting rates and activation barriers. Phys. Rev. Lett. 110, 158105.
[72] Sigdel, K.P., Grayer, J.S. and King, G.M. (2013) Three-dimensional atomic force microscopy: interaction force vector by direct observation of tip trajectory. Nano Lett. 13, 5106–5111.
[73] Mokaberi, B. and Requicha, A.A.G. (2006) Drift compensation for automatic nanomanipulation with scanning probe microscopes. IEEE Trans. Autom. Sci. Eng. 3, 199–207.
[74] Stipe, B.C., Rezaei, M.A. and Ho, W. (1998) Single-molecule vibrational spectroscopy and microscopy. Science 280, 1732–1735.
[75] Ewers, H., Jacobsen, V., Klotzsch, E., Smith, A.E., Helenius, A. and Sandoghdar, V. (2007) Label-free optical detection and tracking of single virions bound to their receptors in supported membrane bilayers. Nano Lett. 7, 2263–2266.
[76] Jacobsen, V., Stoller, P., Brunner, C., Vogel, V. and Sandoghdar, V. (2006) Interferometric optical detection and tracking of very small gold nanoparticles at a water–glass interface. Opt. Express 14, 405–414.
[77] Fernandez, J.M., Chu, S. and Oberhauser, A.F. (2001) RNA structure – pulling on hair(pins). Science 292, 653–654.
[78] Zhuang, X. and Rief, M. (2003) Single-molecule folding. Curr. Opin. Struct. Biol. 13, 88–97.

[79] Aleman, E.A., Lamichhane, R. and Rueda, D. (2008) Exploring RNA folding one molecule at a time. Curr. Opin. Chem. Biol. 12, 647–654.
[80] Schuler, B. and Eaton, W.A. (2008) Protein folding studied by single-molecule FRET. Curr. Opin. Struct. Biol. 18, 16–26.
[81] Liphardt, J., Onoa, B., Smith, S.B., Tinoco, I.J. and Bustamante, C. (2001) Reversible unfolding of single RNA molecules by mechanical force. Science 292, 733–737.
[82] Radmacher, M., Cleveland, J.P. and Hansma, P.K. (1995) Improvement of thermally-induced bending of cantilevers used for atomic-force microscopy. Scanning 17, 117–121.
[83] Sullan, R.M., Churnside, A.B., Nguyen, D.M., Bull, M.S. and Perkins, T.T. (2013) Atomic force microscopy with sub-picoNewton force stability for biological applications. Methods 60, 131–141.
[84] Viani, M.B., Schaffer, T.E., Chand, A., Rief, M., Gaub, H.E. and Hansma, P.K. (1999) Small cantilevers for force spectroscopy of single molecules. J. Appl. Phys. 86, 2258–2262.
[85] Carrion-Vazquez, M., Oberhauser, A.F., Fowler, S.B., Marszalek, P.E., Broedel, S.E., Clarke, J. and Fernandez, J.M. (1999) Mechanical and chemical unfolding of a single protein: a comparison. Proc. Natl. Acad. Sci. U.S.A. 96, 3694–3699.
[86] Hodges, A.R., Bussmann, K.M. and Hoh, J.H. (2001) Improved atomic force microscope cantilever performance by ion beam modification. Rev. Sci. Instrum. 72, 3880–3883.
[87] Maali, A., Cohen-Bouhacina, T., Jai, C., Hurth, C., Boisgard, R., Aime, J.P., Mariolle, D. and Bertin, F. (2006) Reduction of the cantilever hydrodynamic damping near a surface by ion-beam milling. J. Appl. Phys. 99, 024906.
[88] Bull, M.S., Sullan, R.M., Li, H. and Perkins, T.T. (2014) Improved single molecule force spectroscopy using micromachined cantilevers. ACS Nano, http://dx.doi.org/10.1021/nn5010588.
[89] Radmacher, M., Fritz, M., Hansma, H.G. and Hansma, P.K. (1994) Direct observation of enzyme activity with the atomic force microscope. Science 265, 1577–1579.
[90] Yano, T., Ichimura, T., Kuwahara, S., Verma, P. and Kawata, S. (2012) Subnanometric stabilization of plasmon-enhanced optical microscopy. Nanotechnology 23, 205503.
[91] Muller, D.J., Helenius, J., Alsteens, D. and Dufrene, Y.F. (2009) Force probing surfaces of living cells to molecular resolution. Nat. Chem. Biol. 5, 383–390.
[92] Dufrene, Y.F., Martinez-Martin, D., Medalsy, I., Alsteens, D. and Muller, D.J. (2013) Multiparametric imaging of biological systems by force-distance curve-based AFM. Nat. Methods 10, 847–854.
[93] Dufrene, Y.F., Evans, E., Engel, A., Helenius, J., Gaub, H.E. and Muller, D.J. (2011) Five challenges to bringing single-molecule force spectroscopy into living cells. Nat. Methods 8, 123–127.
[94] Fuhs, T., Reuter, L., Vonderhaid, I., Claudepierre, T. and Kas, J.A. (2013) Inherently slow and weak forward forces of neuronal growth cones measured by a drift-stabilized atomic force microscope. Cytoskeleton 70, 44–53.
[95] Marszalek, P.E., Lu, H., Li, H., Carrion-Vazquez, M., Oberhauser, A.F., Schulten, K. and Fernandez, J.M. (1999) Mechanical unfolding intermediates in titin modules. Nature 402, 100–103.
[96] Shaevitz, J.W., Abbondanzieri, E.A., Landick, R. and Block, S.M. (2003) Backtracking by single RNA polymerase molecules observed at near-base-pair resolution. Nature 426, 684–687.
[97] Greenleaf, W.J., Frieda, K.L., Foster, D.A., Woodside, M.T. and Block, S.M. (2008) Direct observation of hierarchical folding in single riboswitch aptamers. Science 319, 630–633.
[98] Yu, H., Liu, X., Neupane, K., Gupta, A.N., Brigley, A.M., Solanki, A., Sosova, I. and Woodside, M.T. (2012) Direct observation of multiple misfolding pathways in a single prion protein molecule. Proc. Natl. Acad. Sci. U.S.A. 109, 5283–5288.
[99] Neuman, K.C. and Nagy, A. (2008) Single-molecule force spectroscopy: optical tweezers, magnetic tweezers and atomic force microscopy. Nat. Methods 5, 491–505.
[100] Greenleaf, W.J., Woodside, M.T. and Block, S.M. (2007) High-resolution, single-molecule measurements of biomolecular motion. Annu. Rev. Biophys. Biomol. 36, 171–190.